the plant journal

SEB Society for Experimental Biology

The Plant Journal (2016) **88,** 963–975 doi: 10.1111/tpj.13306

Interference with ethylene perception at receptor level sheds light on auxin and transcriptional circuits associated with the climacteric ripening of apple fruit (*Malus x domestica* Borkh.)

Alice Tadiello[1,†], Sara Longhi[1,†,‡], Marco Moretto[1], Alberto Ferrarini[2], Paola Tononi[2], Brian Farneti[3], Nicola Busatto[3], Urska Vrhovsek[1], Alessandra dal Molin[2], Carla Avanzato[2], Franco Biasioli[1], Luca Cappellin[1], Matthias Scholz[1,‡], Riccardo Velasco[1], Livio Trainotti[4], Massimo Delledonne[2] and Fabrizio Costa[1,*]

[1]*Research and Innovation Centre, Fondazione Edmund Mach, Via Mach 1, 38010 San Michele all'Adige, Trento, Italy,*
[2]*Department of Biotechnology, University of Verona, Strada le Grazie 15,Verona 37134, Italy,*
[3]*Department of Agricultural Sciences, Bologna University, Via Fanin 46, Bologna 40127, Italy, and*
[4]*Biology Department, Padova University, Viale Giuseppe Colombo 3, Padova 35121, Italy*

Received 15 April 2016; revised 9 August 2016; accepted 11 August 2016; published online 5 October 2016.
*For correspondence: (e-mail: fabrizio.costa@fmach.it).
†Equally contributing authors.
‡Current address: Centre for Integrative Biology (CIBIO), University of Trento, Via Sommarive n. 9 38123 Povo, Trento, Italy.

SUMMARY

Apple (*Malus x domestica* Borkh.) is a model species for studying the metabolic changes that occur at the onset of ripening in fruit crops, and the physiological mechanisms that are governed by the hormone ethylene. In this study, to dissect the climacteric interplay in apple, a multidisciplinary approach was employed. To this end, a comprehensive analysis of gene expression together with the investigation of several physiological entities (texture, volatilome and content of polyphenolic compounds) was performed throughout fruit development and ripening. The transcriptomic profiling was conducted with two microarray platforms: a dedicated custom array (iRIPE) and a whole genome array specifically enriched with ripening-related genes for apple (WGAA). The transcriptomic and phenotypic changes following the application of 1-methylcyclopropene (1-MCP), an ethylene inhibitor leading to important modifications in overall fruit physiology, were also highlighted. The integrative comparative network analysis showed both negative and positive correlations between ripening-related transcripts and the accumulation of specific metabolites or texture components. The ripening distortion caused by the inhibition of ethylene perception, in addition to affecting the ethylene pathway, stimulated the de-repression of auxin-related genes, transcription factors and photosynthetic genes. Overall, the comprehensive repertoire of results obtained here advances the elucidation of the multi-layered climacteric mechanism of fruit ripening, thus suggesting a possible transcriptional circuit governed by hormones and transcription factors.

Keywords: apple, ethylene, fruit ripening, transcription regulation, correlation analysis network, hormonal interplay.

INTRODUCTION

Apple (*Malus x domestica* Borkh.) is one of the most important fruit crops worldwide. This fruit is generally harvested for fresh consumption, and among the 'fleshy fruits', apple has a year-round availability (El-Ramady *et al.*, 2015), primarily enabled by the properties of the cell wall. The cell wall, together with other traits that influence fruit quality, is differentially regulated throughout fruit development and the ripening process. It is during this phase that several physiological pathways related to color, flavor, aroma and texture are prominent (Giovannoni, 2001).

Throughout the ripening of climacteric fruits (such as tomato, banana, peach, kiwifruit and apple), the coordination of these physiological modifications is regulated by the plant hormone ethylene (Yang and Hoffman, 1984; Alexander and Grierson, 2002). Ethylene is a small volatile hormone that, in higher plants, triggers and coordinates several processes, from seed germination to fruit ripening.

In climacteric fruits, the level of ethylene increases from a basal auto-inhibitory level to an auto-catalytic accumulation at the onset of ripening (Yang and Hoffman, 1984; Barry *et al.*, 2000; Bleecker and Kende, 2000). Ethylene is synthesized by the metabolic pathway known as the Yang cycle (Adams and Yang, 1979; Yang and Hoffman, 1984), and is perceived by receptors promoting the expression of a cascade of downstream responsive genes (Ciardi *et al.*, 2000 and Ciardi *et al.*, 2001; Klee, 2002). In the signaling model, receptors act as negative regulators of the ethylene response (Lanahan *et al.*, 1994; Bleecker and Schaller, 1996; Klee, 2002; Wang *et al.*, 2002; Guo and Ecker, 2004). A reduction in receptor content therefore increases the ethylene sensitivity, whereas the kinase cascade is switched off following ethylene binding (Ciardi *et al.*, 2000 and Ciardi *et al.*, 2001). This interaction has been extensively exploited in post-harvest management to extend the storage performance of climacteric fruits, especially apple (Sisler and Serek, 1997). Excessive ripening can in fact lead to dramatic fruit loss, off-flavor and decay (Matas *et al.*, 2009). Deviation from the general ripening condition as a result of interference at the ethylene receptor level was originally observed in the *Solanum lycopersicum* (tomato) mutant *Never ripe* (*Nr*; Hackett *et al.*, 2000; Tieman *et al.*, 2000; Alba *et al.*, 2005). In apple, despite the great diversity in ripening behavior among several accessions, specific ripening mutants are still unknown; however, the application of 1-methylcyclopropene (1-MCP) can mimic the ethylene binding deficiency of *Nr*. This molecule delays the entire ripening process, and is therefore a valuable alternative to dissect the ethylene regulatory network in apple. The role of 1-MCP has previously been investigated in apple (Costa *et al.*, 2010), revealing gene expression changes similar to what was presented in tomato (Alba *et al.*, 2005). In both cases, however, the gene expression survey was performed with a microarray platform (TOM1) harboring only 25% of the tomato gene inventory. Although several other works investigating apple fruit ripening have been presented to the scientific community (Janssen *et al.*, 2008; Soglio *et al.*, 2009; Zhu *et al.*, 2012), it is also true that most of these studies relied solely on gene expression. In this work, an integrative and comparative investigation of transcriptome profiling, together with texture, volatile organic compound (VOC) and secondary metabolite analysis, was conducted, and subsequently a broad systematic picture of the principal mechanisms regulating fruit ripening are described.

RESULTS AND DISCUSSION

Apple fruit development and ripening characterization

The experimental scheme adopted in this work (Figure S1a) was based on a time course, defined by eight stages, designed to span the fruit development and ripening of two apple cultivars, 'Golden Delicious' (GD) and 'Granny Smith' (GS). Five stages represented fruit development (from F to B), whereas the last three stages were mainly related to the maturity/full ripening phase (harvest, H; post-harvest, PH) . To confirm ripening homogeneity, the internal chlorophyll content was assessed with a DA meter (DA: difference of absorbance) (Figure S1b). With regards to fruit size, the I_{AD} index was detected, starting from the stage G. The ripening assessment clearly shows distinct behavior for the two cultivars. The first two samples (G and MG) did not show any relevant change in I_{AD} across stages or between cultivars (based on ANOVA, $P \leq 0.05$). In the second group of samples, although GS showed a slight variation in I_{AD}, a statistically significant change was observed in GD. From B to H, the I_{AD} index decreased approximately 50%, but after 1 week of shelf life, the index dropped by an additional 40%. To interfere with the normal climacteric ripening, 1 mg L^{-1} of the ethylene competitor 1-methylcyclopropene (1-MCP) was applied to a batch of apples collected at stage H. The treatment, according to internal chlorophyll content, effectively delayed the progression of apple ripening in GD. In fact, the I_{AD} index value of the PH-treated sample decreased by only 26% (with regards to stage H), showing a significant difference between the two post-harvest stages (PH_{CTRL}/$PH_{1\text{-}MCP}$) of approximately 20%. The efficacy of 1-MCP in delaying fruit ripening was additionally demonstrated by the measurement of ethylene over a month of shelf life (Figure S1c). As expected, although ethylene remained at a basal level during fruit development, it started to accumulate during stage H, with values of 1120 and 35 nL L^{-1} for PH_{CTRL} in GD and GS, respectively. The application of 1-MCP efficiently suppressed ethylene accumulation in both cultivars. In $PH_{1\text{-}MCP}$, ethylene reached a concentration of approximately 5 nL L^{-1} for GD and 3 nL L^{-1} for GS, resulting in a fold change of 224 and 11.6, respectively. Finally, the assessment of the fruit texture behavior and the production of secondary metabolites (VOCs and polyphenols) are detailed in Appendix S1.

Transcriptional climacteric signatures unravel the physiological change in response to the inhibition of ethylene perception

Apple fruit development and ripening was functionally investigated by measuring the transcript variation with two microarray platforms, iRIPE and WGAA. The first array was employed to profile the transcriptional dynamics over the entire time course, whereas the second array was implemented to better dissect the role of ethylene in climacteric post-harvest ripening. The profile generated with iRIPE was organized into 70 different self-organizing tree algorithm (SOTA) expression patterns, using F as a reference (Figure S2). The iRIPE transcriptome clearly distinguished the physiological behavior of the apple samples, as

depicted by the two-dimensional principal components analysis (2D-PCA) hyperspace plot (Figure 1). Interestingly, in both cultivars the samples treated with 1-MCP showed a transcriptome make-up closer to stage H with respect to the control counterpart. Considering that the two post-harvest samples (PH_{CTRL} and $PH_{1\text{-}MCP}$; Figure S1a) coincide in terms of DAH, their distribution previously demonstrated the physiological modification caused by 1-MCP. The overall transcript regulation was further depicted in two ways. Initially, the gene expression profiles were presented according to heat-map/hierarchical clustering, which assembled the genes on the basis of their expression pattern (Figure 2a). The same transcriptome variation was further illustrated by anchoring the expression of genes to the genome assembly (Figures 2b, c and S3), thus allowing the visualization of the transcriptional changes with regards to genomic regions associated with the variation in fruit texture presented by Longhi *et al.* (2012). Although this is far from a comprehensive genetic genomics study (Janssen and Nap, 2001; Breitling *et al.*, 2008; Joosen *et al.*, 2009), this synergic integration was performed as a first attempt to merge genetic results with gene expression (Li and Burmeister, 2005). Although the transcripts were widely spread over the genome, it is interesting to note that on chromosomes 5, 6, 10 and 15, the gene expression change co-localized with important QTL regions, suggesting the activity of a *cis*-regulating QTL. Of particular interest was chromosome 10, where the highest expression was observed for *Md-PG1*, a gene playing a pivotal role in the control of fruit texture in apple (Costa *et al.*, 2010; Longhi *et al.*, 2012 and Longhi *et al.*, 2013).

Out of the total number of genes investigated with iRIPE, 675 were differentially expressed ($P \leq 0.05$, fold change ≥ 2) in at least one pairwise comparison in GD (Figure S4; Table S1). The highest numbers of differentially expressed genes (DEGs) were identified in the F/L

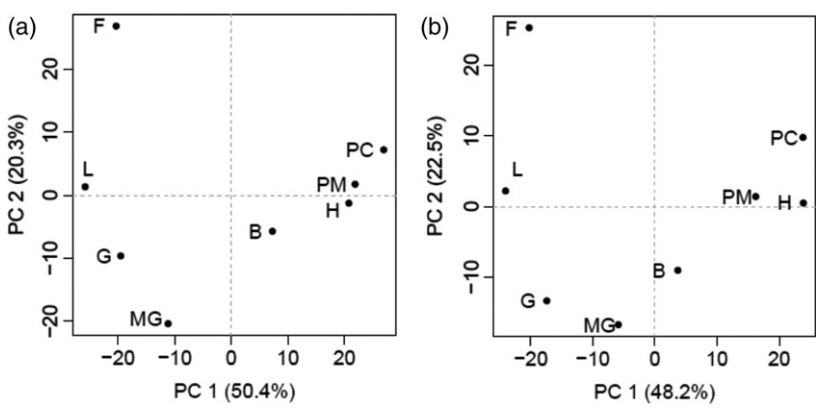

Figure 1. Two-dimensional principal components analysis (2D-PCA) plot depicting the distribution of several samples on the base of their transcription pattern assessed with the iRIPE array. The PCA plot is distinguished by the first two principal components for (a) 'Golden Delicious' and (b) 'Granny Smith'. In each panel the samples are coded as: F, flower; L, fruitlet; G, green; MG, mature green; B, breaker; H, harvest; PC, post-harvest control; PM, post-harvest treated with 1-methylcyclopropene (1-MCP).

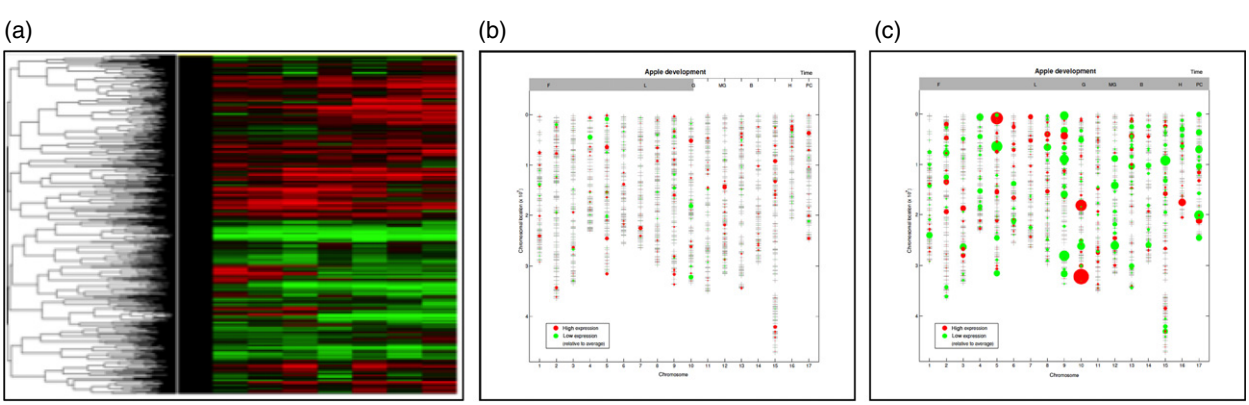

Figure 2. iRIPE overall transcription profile assessment. (a) Dynamics represented according to a hierarchical heat map clustering. Samples are ordered on the basis of time course (coding is the same as described in Figure 1) and anchored to the flower stage. The other two panels show the expression profile of the genes aligned on the genome, and are representative snapshots for the green (b) and the post-harvest control (c) stages. For the three representations, green and red represent low and high gene expression, whereas the expression magnitude is highlighted by the size of the dots in panels (b) and (c).

comparison, followed by the MG/B and B/H, which is evidence of the physiological shift from the end of fruit development to horticultural maturity. This regulation, as clearly shown in the MapMan visualization (Figure S5a), highlights, for instance, the downregulation of genes involved in the light reaction process, such as light-harvesting chlorophyll *a*/*b* binding proteins. This physiological variation suggests that the change from MG to B is the transition from the partial photosynthetic source to the heterotrophic sink (Jones, 1981). This functional shift was also observed in other climacteric fruits, such as tomato, where photosynthetic light reaction-related genes were upregulated in the early developmental phase and downregulated in late fruit ripening stages (Carrara *et al.*, 2001; Lytovchenko *et al.*, 2011; Rohrmann *et al.*, 2011; Osorio *et al.*, 2012). It is also worth noting the de-repression of the photosynthetic light reaction machinery following 1-MCP treatment. Whereas two genes were re-activated (MDP0000233260 and MDP0000836781) in GD, almost the entire set involved in the light reaction machinery was de-repressed in GS. This specific positive stimulation generated by the ethylene inhibitor was further magnified in the WGAA transcriptomic overview (Figure S5b). This finding is in agreement with results observed in the tomato *Nr* mutant, which showed an induction of the expression of photosynthetic-related genes that are normally downregulated during ripening (Osorio *et al.*, 2011). The shift from B to H is instead more related to the initiation of the climacteric process, as the genes involved in ethylene regulation were strongly activated in the latter stage, including the well-documented elements involved in ethylene biosynthesis and the signal transduction pathway (*ACS*, *ACO* and *ERF2*). The impact of ethylene in controlling the climacteric ripening was dissected here with the use of the ethylene competitor 1-MCP. As expected, the interference at the receptor level determined an important repression of genes involved in the ethylene pathway (*ACS*, *ACO*, *ETR* and *ERF*). Despite the downregulation of 61.8% of the genes differentially expressed between control and treated samples, it is also worth noting the positive regulation of 38.2% of the gene set, for which most are represented by transcription factors (*MADS*, *NAC*, *AUX/IAA* and *ERF*) and elements involved in the chlorophyll machinery (light harvesting, chlorophyll *a*/*b* binding proteins). The double effect of ethylene during ripening was additionally investigated in more detail using the WGAA array, which improved the transcriptome resolution in the last three stages (H, PH_{CTRL} and $PH_{1\text{-}MCP}$). The different fruit ripening physiology of these samples was clearly depicted in the 2D-PCA plot (Figure 3a), together with the heat-map hierarchical clustering (Figure 3b,c). From the total set of 46 098 genes represented on the whole genome array, 7106 were differentially expressed in the two pairwise sample comparisons of the GD cultivar. In the PH_{CTRL}/H comparison, 4771 DEGs were identified, of which 58.1% were expressed in the PH sample and 41.9% were expressed in the H sample (Table S2a). In the $PH_{1\text{-}MCP}$/PH_{CTRL} comparison, 4335 DEGs were identified, of which 55% were highly expressed in the

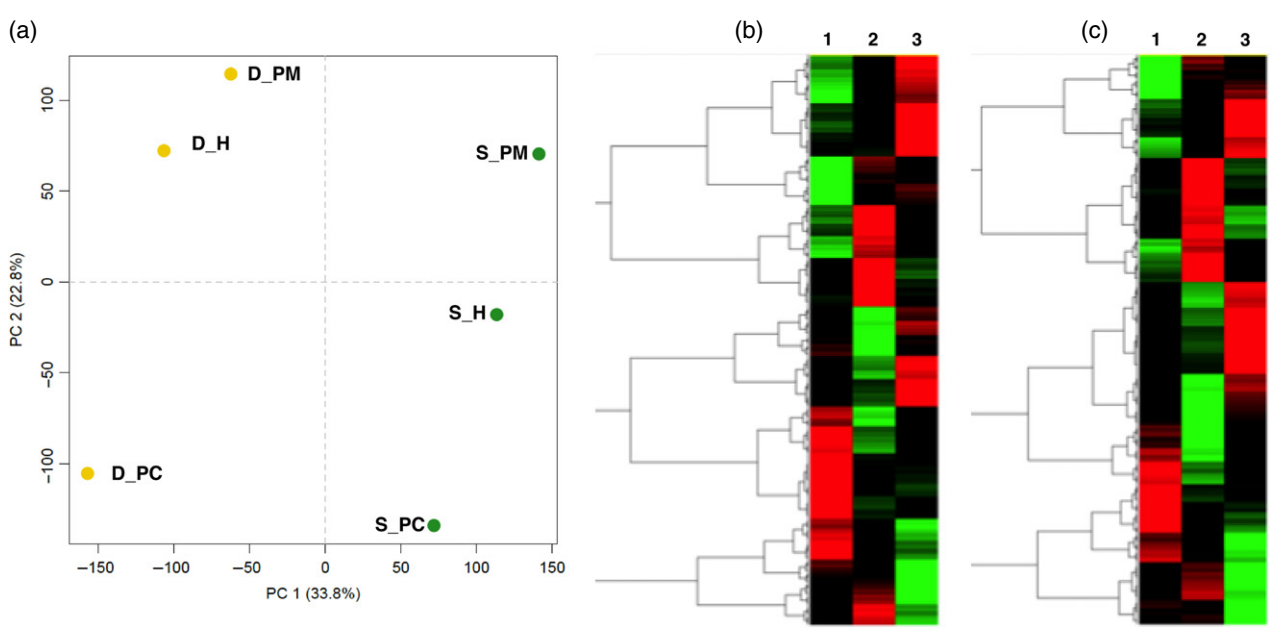

Figure 3. Gene expression profile assessed with the WGAA platform in the two apple cultivars. (a) Distribution of the last three samples of the time course (harvest, post-harvest control and treated) over the two-dimensional principal components analysis (2D-PCA) plot. (b, c) Expression dynamics depicted with a hierarchical heat-map clustering for 'Golden Delicious' (D) and 'Granny Smith' (S), respectively. In both heat maps the samples are depicted as follows: harvest (1), post-harvest control (2) and post-harvest treated with 1-methylcyclopropene (1-MCP) (3).

sample treated with 1-MCP, compared with the control (45%), sharing 2000 common genes (Table S2b).

The gene expression profile of the two microarray platforms was validated by RT-qPCR. The pairwise correlation (higher than 0.50; $P < 0.05$) shown in Figure S6 confirmed the reliability among the different methodologies employed here.

Ripening regulation in two apple cultivars, 'Golden Delicious' and 'Granny Smith'

The transcriptome variation assessment allowed the physiological cross-comparison between two apple cultivars, represented by GD, showing a typical climacteric behavior (and considered the reference cultivar), and GS, known to produce a much lower quantity of ethylene with a consequential reduced progression of cell wall dismantling. Initially, the iRIPE genomic platform was employed to monitor the overall transcriptomic signature between the two cultivars. Over the time course, however, significant gene expression differences only arose from the MG stage onwards, because at stage G the two cultivars were transcriptionally identical (no DEGs were found). At stage MG, the number of DEGs was 78, with 60 transcripts more abundant in GD and 18 transcripts more abundant in GS, among which a high number of transcription factors (TFs) and secondary metabolite genes were identified (Figure S7; Table S3a). In stage B, an opposite trend was observed, with a greater number of genes showing increased expression in GS (Figure S7; Table S3b). At stage H, the functional state between the two apple cultivars was similar (55 DEGs in GS and 66 DEGs in GD; Figure S7; Table S3c), although a distinct hormonal signature was detected. In GS, auxin-related genes were predominantly expressed with regards to elements belonging to the hormone ethylene. In fact, in this apple cultivar, four *AUX/IAA*, two *IAA amidohydrolase*, two *ACO* and one *ERF* were identified. In GD, however, none of the auxin-related elements were identified, whereas genes involved in the ethylene biosynthetic and regulation pathway were more abundant, such as two *SAM*, two *ACS*, six *ACO*, two *ETR* and three *ERF* elements (Table S3c). This scenario was magnified in the post-harvest comparison ($PH_{CTRL}/PH_{1\text{-}MCP}$; Figure S7; Table S3d). The hormonal distinction between the two cultivars is supported by the higher rate of ethylene produced by GD at this stage and ethylene-mediated genes, in particular those related to cell wall metabolism. Among these, it is also worth noting the identification of three *endo-xyloglucan-transferase*, two *expansins* and one *polygalacturonase* element. The interference of ethylene physiology, as a result of treatment with 1-MCP, re-shaped the functional regulation between the two cultivars (Figure S8; Table S3e). The ethylene inhibitor induced the expression of twice the number of genes in GS compared with GD (66 and 31 DEGs, respectively). In particular, in GS a high number of light-harvesting chlorophyll *a*/*b* binding protein and several transcription factor elements (*ERF*, *MADS* and *NAC*) were upregulated. The comparison between the two cultivars was further investigated using the WGAA platform, which allowed for a more detailed investigation of the climacteric phase (Figure 3). At stage H, the number of DEGs involved in cell wall disassembly was higher in GD (61) than in GS (34), highlighting a more intense polysaccharide disassembling activity in the first cultivar, consistent with the observed texture profile (Figure S8a; Table S4a). Although the numbers of DEGs were almost identical in terms of ethylene regulation (nine in GD and seven in GS; Figure S8b; Table S4b), this was not the case for genes related to the auxin pathway. As previously observed, auxin-mediated genes were highly expressed in the GS cultivar (19), compared with GD (15; Figure S8c; Table S4c). This finding is consistent with the transcriptional overview depicted for transcription factors, which resulted in more genes transcribed in GS (120) than in GD (104; Figure S8d; Table S4d). After 1 week of shelf-life ripening, the transcriptional pattern remained fundamentally unchanged for the cell wall and auxin pathway with respect to stage H. At this stage, in fact, the number of cell wall genes with increased expression was 50 in GD and 31 in GS (Table S4e), whereas the number of upregulated auxin-related transcripts was higher in GS (19) compared with GD (14; Table S4f). The genotype effect between the cultivars on ethylene regulation was confirmed by the different proportion of genes identified using the WGAA platform. Among the ethylene-related DEGs, 12 were highly expressed in GD (Table S4g), but only five were observed in GS. In contrast, the transcription machinery involved in gene regulation processes was quite similar between the two cultivars, with the identification of 93 and 96 transcription factors showing increased expressed in GD and GS, respectively (Table S4h). The deviation from the normal climacteric ripening physiology generated by treatment with 1-MCP was particularly evident in two gene categories: ethylene and cell wall-related genes. Compared with PH_{CTRL}, in $PH_{1\text{-}MCP}$ a reduction in DEGs was observed in both GD and GS. GD showed a reduction of 36% of cell wall genes and 41% of ethylene-related genes, whereas the number of DEGs detected at stage $PH_{1\text{-}MCP}$ was rather similar or slightly higher than at stage H in GS (Table S4i, l). In contrast, concerning the auxin pathway genes, the number of DEGs did not substantially change from the comparison performed between the apple cultivars at the PH_{CTRL} stage, with GS showing a higher number of DEGs than GD (Table S4m). The application of the ethylene competitor led to a slight reduction in the number of TFs expressed in both cultivars, with 88 DEGs expressed in GS and 78 DEGs expressed in GD (Table S4n).

Exogenous application of the ethylene competitor 1-MCP induces a de-repression and activation of the regulatory machinery complex

The competition exerted by 1-MCP binding to receptors instead of ethylene activates a transcriptional circuit affecting the entire fruit-ripening physiology. During normal climacteric ripening (H/PH_{CTRL}; Table S5), 181 DEGs were identified, of which 89 were more highly expressed at the onset of the ethylene burst. With the application of 1-MCP, 184 elements were instead differentially expressed. In this comparison, however, the majority of the genes in the 1-MCP-treated sample (111) were positively stimulated by the inhibition of the ethylene accumulation and signaling. Among the class of transcription factors (Table S5), several families were stimulated by 1-MCP, such as *NAC domain*, *MADSbox* and elements involved in the auxin regulatory process (*AUX/IAA*). Treatment with 1-MCP stimulated the expression of approximately 60% of the transcription factors, possibly as a mechanism to restore the normal physiological ripening condition. This hypothesis is also supported by the fact that most of the genes induced by 1-MCP, besides TFs, are auxin- and ethylene-related genes, in addition to those involved in the photosynthetic pathway. The molecular interplay between regulatory elements and the two major plant hormones constitute the core of fruit-ripening control mechanisms (Tieman *et al.*, 2000; Giovannoni, 2001). The role of transcription factors has been previously demonstrated in coordinating the ethylene burst during ripening (reviewed in Klee and Giovannoni, 2011). In this particular case, it is also worth noting that amongst the list of TF elements stimulated by the treatment, *NAC* (one of the most abundant TF families in the plant genomes sequenced to date) and *zinc finger* are the most represented (Figure 4). In tomato, the important role played by *NAC* factors in several biological processes, from plant growth and development to fruit ripening, has been demonstrated (Giovannoni, 2007; Zhu *et al.* 2014). Indeed, *SlNAC* accumulates in fruit tissues with an

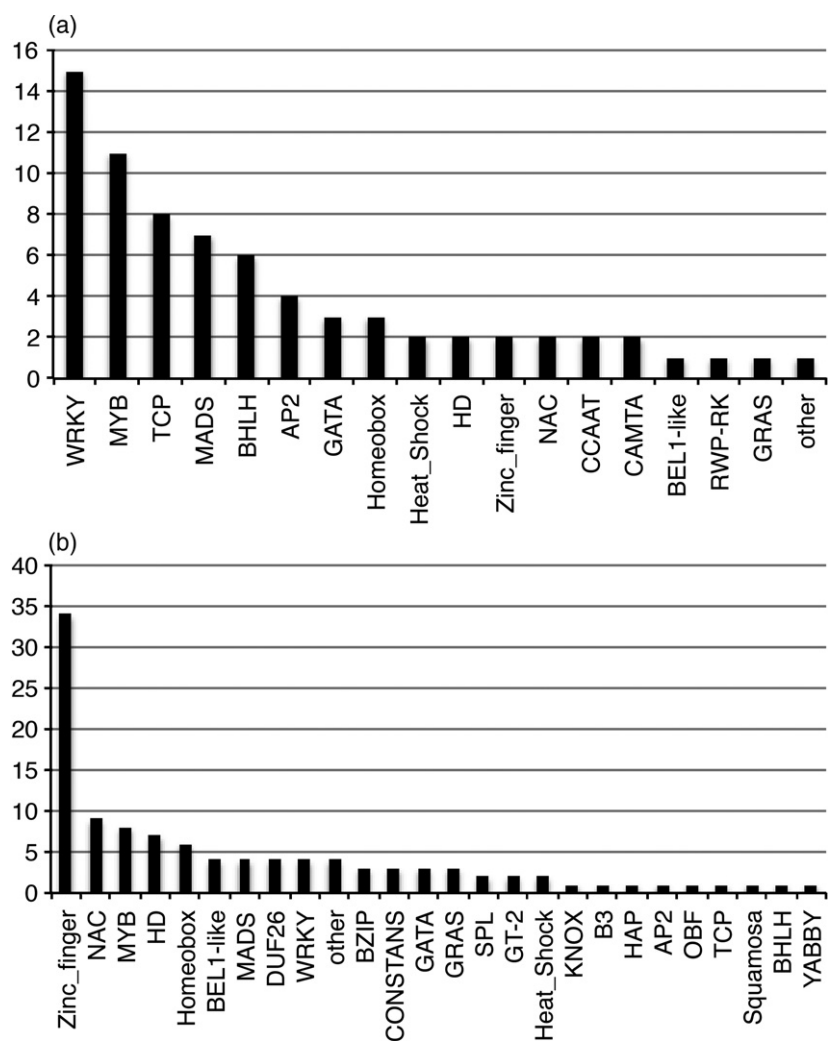

Figure 4. Distribution of the transcription factor genes identified with the WGAA platform and differentially expressed in the control (a) and 1-methylcyclopropene (1-MCP)-treated (b) postharvest samples.

increased expression pattern throughout fruit ripening. In the work of Ma *et al.* (2014), an *NAC* factor, namely *SlNAC1*, seemed to function as a negative regulator of fruit ripening because a transgenic tomato line overexpressing this gene showed inhibited fruit ripening. In addition, Xie *et al.* (2000) reported a relationship between *NAC* and auxin. *NAC1* expression is in fact induced by auxin, and auxin-responsive genes were identified and recognized as downstream targets of *NAC1*. This functional interaction shed light on the hypothesis formulated here concerning the mechanism triggered by the application of 1-MCP, and was additionally supported by the different ripening behavior of the two apple genotypes. Blocking ethylene sensitivity at the receptor level switched off ethylene production, stimulating the expression of *NAC* elements and the subsequent activation of the auxin pathway in an attempt to re-establish normal ethylene physiology. In this work, the application of 1-MCP has helped to decipher more accurately the ethylene network, suggesting a possible transcriptional circuit controlled by hormone and TFs in the regulation of apple fruit ripening. According to BLAST results, the apple *NAC* (MDP0000404409) shows 96% nucleotide and 61% peptide sequence similarity with *NAC1* in tomato (Solyc06g060230.2), thus suggesting a putative orthologous relationship.

Interference of ethylene perception during the last phase of fruit ripening stimulates a hormonal interplay with auxin

The ethylene-mediated transcription and relative functional deviation caused by 1-MCP were depicted in three MapMan classes (Figure S4, 5). The physiological effect of the exogenous application of the ethylene competitor 1-MCP was clear in the regulation of ethylene. The DEGs related to this hormone were in fact more highly expressed in PH_{CTRL} compared with $PH_{1\text{-}MCP}$ (Table S5c,d). In addition, however, the application of 1-MCP also stimulates the activation of genes involved in other fundamental pathways of fruit ripening. In addition to light regulation, it is also interesting to note the upregulation observed in the auxin pathway. In the H/PH_{CTRL} comparison 30 DEGs were detected (almost equally present in the two samples, with 14 and 16 expressed at H and PH_{CTRL}, respectively; Table S5e), and 31 DEGs were identified after treatment with 1-MCP (Table S5f), highlighting an almost un-modified physiological state. Among this set, 1-MCP stimulated a similar number of elements compared with those expressed in the presence of ethylene. In fact, of the 16 genes potentially regulated during the climacteric ripening, 15 were more highly expressed after 1-MCP application, such as *IAA auxin induced protein*.

To unravel this transcriptional circuit controlling climacteric ripening in apple, a correlation analysis network (CAN) was performed. As an initial attempt to highlight the distortion generated by the ethylene antagonist, a comparative network was generated between the iRIPE interactome and the accumulation of ethylene (Figure 5a, b). Treatment with 1-MCP changed the ethylene interactome by approximately 2.8-fold. Whereas during normal ripening the ethylene trend was correlated with 69 genes (34 negative and 35 positive interactions; Table S6a), in samples treated with 1-MCP a total of 24 interactions were observed (nine negative and 15 positive; Table S6b). Among the genes negatively correlated with ethylene in normal ripening physiology, enrichment in auxin-related genes was observed, such as *AUX/IAA*, *TIR1* and two *ARF* elements. In contrast, within the gene set showing a positive interaction with ethylene, several ethylene-related

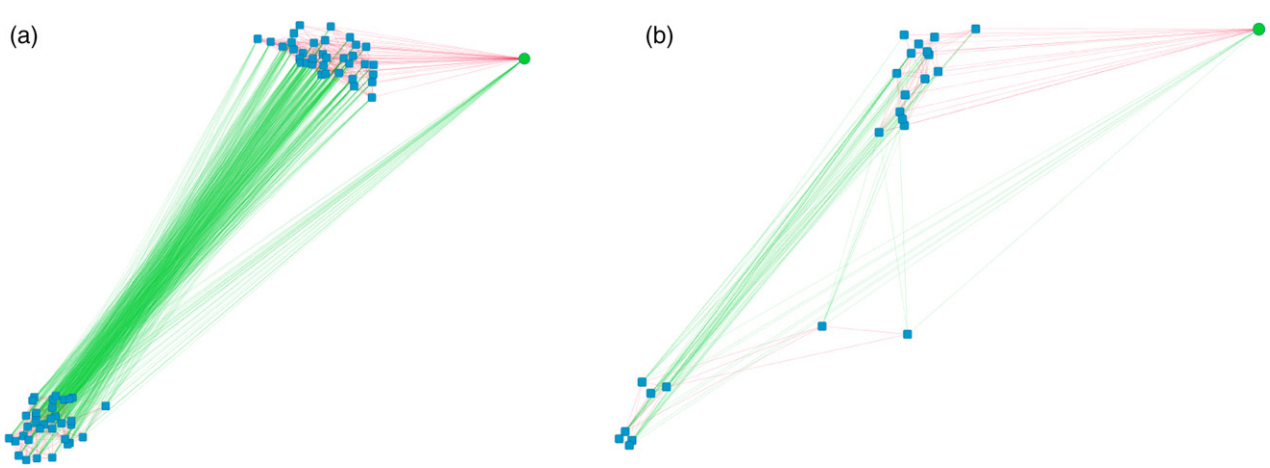

Figure 5. Visualization of the transcript–ethylene correlation network. The cluster is the selection of the gene transcription pattern positively and negatively correlated with the hormonal accumulation. Positive correlations are indicated with red edges, whereas negative correlations are displayed in green. Nodes are of two types: ethylene is indicated with a green circle, whereas transcripts are represented by blue squares. Panels (a) and (b) show the correlation defined under normal climacteric conditions and with the inhibition of ethylene hormone perception, respectively.

genes (such as *ACO* and *ERF*) and cell wall modifying genes (*PME*, *PG* and *endoxyloglucan transferase*) were identified. Among this set, a *GH3* involved in the IAA conjugation process was identified. In the correlation network analysis performed with the ethylene profile in the physiologically distorted scenario (treated with 1-MCP), within the group of the transcripts positively regulated, several elements involved in the ethylene signaling and perception machinery (such as *ERS* and *ERF*) were identified, whereas among the genes negatively regulated, three *AUX/IAA* elements were instead identified. The network analysis performed with the iRIPE was also consistent with the more comprehensive correlation analysis conducted using the WGAA platform. The transcript dynamics profile was positively correlated with a series of genes largely involved in ethylene biosynthesis and the signaling mechanism, such as *ACO*, *ACS*, *AP2-ethylene responsive factor* and *ERF* (Table S7a). As previously observed with the iRIPE platform, it is also interesting to note the identification of elements involved in the auxin pathway, such as *AUX/IAA* and GH3; however, the majority of the genes related to the auxin pathway were negatively correlated compared with ethylene accumulation, such as *ARF*, *Auxin transporter*, *AUX/IAA* and *PIN auxin efflux transporter*. The presence of these specific classes of auxin-related genes leads us to hypothesize that a possible link with ethylene in apple fruit exists. These two hormones have been previously shown to act both synergistically and antagonistically in several physiological processes (Muday *et al.*, 2012). *ARF* transcription factors and *AUX/IAA* are two classes of regulators triggering the expression of auxin-responsive genes (Lokerse and Weijers, 2009; Leyser, 2010), and because auxin is more involved in early fruit developmental processes, the time of ripening correlates with a decrease in its concentration and action (Schaffer *et al.*, 2013; Shin *et al.*, 2016). As reported in tomato, although the expression of auxin-responsive genes was strongly reduced during the ripening process in wild-type plants, an induction was observed in the *Nr* mutant deficient in ethylene perception (Osorio *et al.*, 2011). The modulation of the auxin pool, aside from the regulation of *de novo* synthesis, is also controlled by a conjugation/degradation mechanism (Ljung, 2013), contributing to auxin homeostasis and storage (Chapman and Estelle, 2009). The idea of an ethylene–auxin interplay at a late ripening stage is moreover validated by the systemic analysis performed with samples treated with 1-MCP. The activation of *AUX/IAA* and *ARF* elements is moreover consistent with the findings that a high auxin level can stimulate the synthesis of ethylene in the late fruit ripening phase (Morgan and Hall, 1962; Trainotti *et al.*, 2007). In this scenario, the auxin–ethylene interplay might play a role. Because ethylene production by the fruit is inhibited by impaired perception, the auxin pathway is stimulated as a parallel metabolism mechanism to restore the normal climacteric physiology (Figure 6).

Correlation analysis network reveals an association between transcripts and phenomic entities

The class of genes encoding cell wall modifying proteins (CWMPs) was also strongly affected by treatment with 1-MCP (Figure S5). In the H/PH_{CTRL} comparison, 58 genes out of 70 were more highly expressed in the presence of ethylene (Table S5a). After treatment with 1-MCP, the majority of the genes encoding cell wall enzymes (50 of 77) were, as expected, repressed (Table S5b), such as *polygalacturonase*, *pectinesterase* and *pectate lyase*; however, treatment with 1-MCP also stimulated a specific set of cell wall-related genes, with most belonging to the *xyloglucan endo-transglycosylase* family. In the CAN analysis performed with texture parameters, the application of 1-MCP increased the number of interactions with both mechanical and acoustic parameters (Figure S9a; Table S6c). The mechanical properties in fact showed 537 interactions in the control sample and 657 interactions in the sample treated with 1-MCP (Figure S9a; Table S6d). Similarly, the acoustic parameters showed 140 interactions in the control sample (Figure S9a; Table S6e) and 622 interactions in the sample treated with the ethylene competitor (Figure S9a; Table S6f). This trend was also confirmed by the WGAA platform, which identified 2045

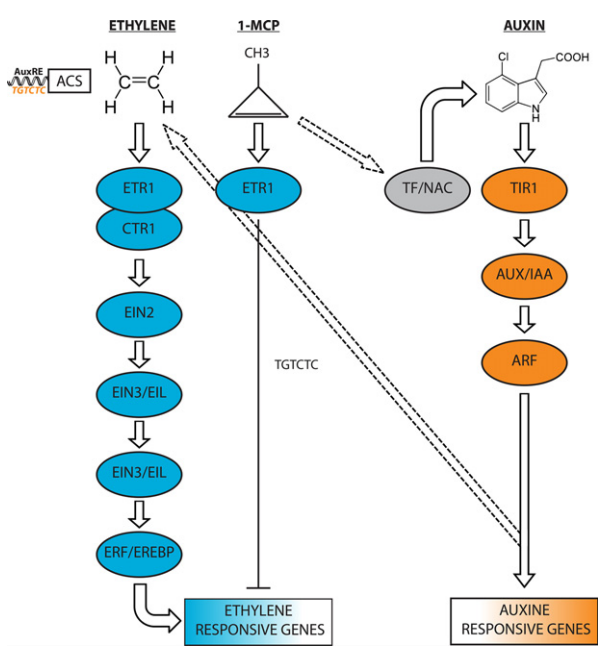

Figure 6. Visual representation of the biochemical pathway of ethylene (blue color) and auxin (orange color). Interference arising from treatment with 1-methylcyclopropene (1-MCP) is also illustrated for the ethylene pathway, and the dashed arrow suggests the point of interaction between the two hormones.

positive and 3025 negative interactions (Table S7b). Although the change in fruit texture in apple has been widely recognized as an ethylene-dependent process, treatment with 1-MCP substantially modified the genes correlated with the phenomenon, rather than the number of interactions. The major difference observed in the two correlation analyses is the expression of *PG* elements in the control sample. This finding is consistent with the role of *polygalacturonase* genes (cleaving the α-1,4-linkage between galacturonic acid residues) in the fruit softening process (Sitrit and Bennett, 1998). Although *PG* was considered important, a *PG*-silenced transgenic line showed only a slight reduction in cell wall degradation (Kramer *et al.*, 1992; Langley *et al.*, 1994; Bennett and Labavitch, 2008). Treatment of melon fruit with 1-MCP has, however, unraveled the different expression patterns of genes encoding CWMPs (Rose *et al.*, 1998; Nishiyama *et al.*, 2007). The use of transgenic lines with suppressed expression of ethylene-related genes in both apple and melon (Dandekar *et al.*, 2004; Ezura and Owino, 2008; Pech *et al.*, 2008) have supported the hypothesis concerning the coexistence of both ethylene-dependent and -independent pathways (Nishiyama *et al.*, 2007). Blocking ethylene by 1-MCP has in fact stimulated the expression of other cell wall genes, such as *expansin*, *endoxyloglucan-transferase* (*EXT*), *pectinesterase* and β-*galactosidase*. The high number of interactions with *endoxyloglucan-transferase* found in samples treated with 1-MCP suggests that this CWMP is a key regulator of fruit crispness in apple. In the primary cell wall architecture, xyloglucan is the principal component of the polymeric matrix (Nishitani and Tominaga, 1992; Nishitani, 1995; Han *et al.*, 2015). This hemicellulose is involved in the maintenance of cell wall rigidity by strengthening the skeletal network with cellulose microfibrils. In this scenario, *EXT* catalyzes the molecular grafting between xyloglucan molecules, interweaving or reconstructing the cell wall matrix. Together with cell wall strength, the crispness response of a fruit cell also depends on the level of hydrostatic pressure (or internal cellular turgor). To this end, it is worth noting that 1-MCP also stimulates the expression of several *aquaporins* encoding water channels, which regulate the hydrostatic pressure that maintains turgor pressure (Maurel, 1997; Mut *et al.*, 2008; Reuscher *et al.*, 2013; Chaumont and Tyerman, 2014).

During the progression of fruit ripening, a blend of aromatic compounds is produced. In this work, the apple volatilome was profiled with proton transfer reaction time-of-flight mass spectrometry (PTR-ToF-MS), and because fruit volatile production is highly correlated with ethylene (Schaffer *et al.*, 2007), the assessment of VOCs was focused on three specific stages: H, PH_{CTRL} and $PH_{1\text{-}MCP}$ highlighting in particular the effect of 1-MCP. The PH_{CTRL} stage of GD was clearly distinguished over the 2D-PCA plot (Appendix 1), following the orientation of the entire volatile set. This sample, when compared with the others, was characterized as having the highest levels of ethylene production. The volatilome analysis also highlighted a qualitative distinction between the two cultivars. From the VOC variability distribution, the three samples of GS are in fact positioned in the upper part of the PC2 positive quadrants, whereas those belonging to GD are more oriented towards the negative section, because of the dominant accumulation of esters and alcohols in this cultivar. The impaired production of ethylene resulted in a strong repression in the emission of VOCs, as described by Farneti *et al.* (2014), and is consistent with the ethylene-dependent relationship reported for melon (Pech *et al.*, 2008). Among the several VOC categories, alcohols and esters were affected most by the treatment, decreasing by 57 and 52%, respectively. The other volatiles, such as carbonyl compounds, general fragments and other unknown compounds, showed a much lower reduction (approximately 20%). This observation indicates that only specific steps of the VOC pathway are controlled by ethylene, a finding that is consistent with previous studies (Defilippi *et al.*, 2005; Schaffer *et al.*, 2007), and demonstrates that in ethylene-suppressed apple, only esters and alcohols are effectively reduced. As revealed through the systemic analysis performed with the iRIPE platform, treatment with 1-MCP reduced the general interactome (Figure S9b) from 352 interactions (observed in the normal physiology for the five VOC categories; Table S6 g) to 227 interactions (Table S6 h). Although 1-MCP negatively modified the number of transcript–compound interactions, alcohol and esters were affected the most. Interactions were reduced by 57 and 52%, respectively, for alcohol and esters in the $PH_{1\text{-}MCP}$ sample, which was further confirmed by WGAA (Table S7c).

Although a considerable number of studies have attempted to understand the genomic effects of fruit development in different species, knowledge of the physiological shift in important secondary metabolites during fruit maturity and ripening is still limited, despite their significant impact on human health and diet (Dillard and German, 2000; Kaur and Kapoor, 2001;Liu, 2004; Hyson, 2011). In this study, seven groups of polyphenolic compounds were investigated and were shown to be highest in accumulation at the G stage. The trend observed here and shared by the two apple cultivars is also consistent with the polyphenolic pattern previously described for other species. In fact, fruits of *Olea europaea* (olive; Alagna *et al.*, 2012) and *Eriobotrya japonica* (loquat; Ding *et al.*, 2001) showed the highest concentrations of polyphenolic compounds in young fruit. Interestingly, in loquat fruit, hydroxycinnamic acid (especially chlorogenic acid, the major polyphenolic compound in ripe fruits) slightly accumulates in the final ripening phase, similar to what has been elucidated here. Although polyphenolic compounds decrease steadily during fruit development and maturation, it is

intriguing to note their relationship with ethylene. In both apple cultivars, the entire set of polyphenolic compounds increased after harvest, concomitantly with the initiation of the ethylene burst. Moreover, this pattern is similar to the previous indication reported for apple (Hoang *et al.*, 2011) and tomato (Tohge *et al.*, 2014). The positive regulation with ethylene was also partially verified by treatment with 1-MCP, although we must consider the limited effects in controlling each compound, which were characterized, moreover, by their behavior. Within the group of secondary metabolites considered here, including hydroxycinnamic acid, dihydrochalcones, flavonols, flavan-3-ol and stilbenes, all except stilbenes showed a higher ratio of genes positively regulated by ethylene progression, whereas stilbenes showed a higher number of interactions negatively correlated with hormone accumulation (Table S7d).

In this work we shed light on the climacteric ripening control in apple by applying the ethylene competitor 1-MCP. The entire life cycle of a plant is governed by hormonal interplay, and whereas auxin is needed for fruit growth, ethylene controls and coordinates the onset of the fruit-ripening phase. In apple, the reduction of auxin and its homeostasis can activate the expression of ethylene biosynthetic-related genes (Shin *et al.*, 2016). Fruit with impaired and deficient ethylene production de-repress a series of developmentally regulated genes. In parallel with the repression of ethylene-related genes, an increased expression of auxin and transcription factor (especially *NAC*) elements was observed in an effort to stimulate the ethylene pathway. To this end, only when the proper quantity of ethylene has accumulated, and been perceived, can VOC-related and ethylene-dependent CWMP-encoding genes be transcribed, contributing to the completion of the fruit ripening process.

EXPERIMENTAL PROCEDURES

Plant material

Fruit from GD and GS apple cultivars were collected over a time course organized to characterize fruit development and ripening. Prior to harvest, fruit samples were collected at five specific pomological stages (Figure S1a): i_Flower (F; 0 days after full bloom, DAFB), ii_Fruitlet (L; 20 DAFB), iii_Green (G; 45 DAFB), iv_Mature Green (MG; 75 DAFB) and v_Breaker (B; 105 DAFB). After this, fruit collection progressed following different harvesting dates. Fruit from GD and GS were harvested (H) at 143 and 171 DAFB, respectively. At this time point, two batches of fruit/variety were collected: one was treated overnight with 1 mg L^{-1} of 1-MCP, whereas the second was maintained untreated as a control (CTRL). After treatment, samples were further taken after 1 week of post-harvest (PH) shelf-life ripening (at room temperature, 20°C) at 150 and 178 DAFB for GD and GS, respectively. The collected fruit were further used for transcriptome analysis as well as physical and metabolite screening. For each point, 15 apples were collected from 10 selected trees/cultivar. The homogeneity of each apple/sampling was verified with a DA meter (Nyasordzi *et al.*, 2013), a portable vis-spectrometer device designed to assess ripening in a non-destructive manner. For each sampling, 10 apples were used for the non-destructive volatile monitoring, followed by destructive texture analysis. The other five apples were instead used for transcriptome and metabolite profiling, for which flesh cortex was processed in the presence of liquid nitrogen, ground and stored at −80°C.

Fruit texture assessment

The change of fruit texture, considered as the simultaneous combination of both mechanical and acoustic signature, over the fruit development and ripening, was assessed with a TAXT*plus* texture analyzer (Stable MicroSystem Ltd, http://www.stablemicrosystems.com) equipped with an Acoustic Envelope Device (AED). For each sample, 20 measurements were performed, represented by four biological replicates (different apples collected from the same cultivar) and five technical replicates (flesh discs obtained by the same fruit), according to the protocol described in Costa *et al.* (2011 and) Costa *et al.* (2012). The combined profile was further used to digitally identify 12 parameters (Table S8).

Volatile organic compound (VOC) monitoring

During fruit developmental stages (from G to B), as well as full ripening (H and PH), VOCs were measured with a commercial PTR-ToF-MS 8000 instrument (Ionicon Analytikal GmbH, http://www.ionicon.com). For the analysis, each sample was placed in a glass jar (1000 ml) provided with two Teflon silica septa on the opposite site. Samples were incubated in a water bath for 30 min at 30°C and measured by a direct injection of the headspace mixture into the PTR-ToF-MS drift tube via a heated peak inlet (110°C) for 30 s, acquiring 30 averaged spectra. The sampling time per channel in the ToF analyzer was 0.1 ns, amounting to 350 000 channels for mass spectrum, with an m/z ranging from 10 to 400, and operated with the following conditions in the drift tube: drift voltage 600 V, 110°C and a pressure of 2.25 mbar. Each single spectrum is the sum of 28 600 acquisitions lasting for 35 μs each. Among the several compounds detected by PTR-ToF-MS, m/z 28.03 corresponded to ethylene, as reported in Costa *et al.* (2014).

Secondary metabolite investigation

Polyphenols were extracted with a water/methanol-chloroform solution, as described in Vrhovsek *et al.* (2012). A volume of 10 ml was filtered with a 0.2-μm PTFE filter prior to ultra-performance liquid chromatography with a Waters Acquity UPLC system (Waters, http://www.waters.com) coupled to a Waters Xevo TQMS in electrospray ionization (ESI) mode. The separation of the phenolic compounds was achieved on a Waters Acquity HSS T3 column (1.8 μm, 100 mm × 2.1 mm) kept at 40°C. In the end, 2 μl was injected into the instrument by an autosampler at a temperature of 6°C. Data were processed with Waters MassLynx 4.1 and TARGETLYNX. The phenolic compounds detected were grouped into six main categories: hydroxycinnamic acids, dihydrochalcones, flavan-3-ols, stilbenes, flavonols and aldehyde.

Transcriptome analysis

For both microarray platforms (iRIPE and WGAA), total RNA was isolated from fruit cortex tissue of three biological replicates with the Spectrum Total RNA kit (Sigma-Aldrich, https://www.sigmaaldrich.com). RNA quantity and quality was controlled with a Nanodrop ND-8000 (ThermoFisher Scientific, http://www.thermofisher.com) and an Agilent 2100 Bioanalyzer (Agilent, http://

www.agilent.com). For the transcriptome analysis carried out with iRIPE, 2 μg of RNA was further amplified and labeled using the RNA ampULSE kit (GEA-022, Kreatech; Leica Biosystems, http://www.leicabiosystems.com). Purified aRNA (4 μg) was subsequently hybridized on the array, following the manufacturer's instructions. After hybridization, microarray slides were scanned using an AxoGenePix 4400A (Molecular Devices, http://www.moleculardevices.com). Densitometric analyses were performed in GenePixPro 7 (provided with the instrument). Probe signals were considered when higher than negative control, based on *Bacillus anthracis* strain 2002013094 (CP009902.1), *Haemophilus ducreyl* strain CLU5 (CP011227.1) and *Alteromonas phage* strain PM2 (AF155037.1) sequences, plus twice the standard deviation. All values were log-transformed (base 2) and quantile-normalized using limma R (Ritchie *et al.*, 2015). Mean values were calculated for replicates, whereas the median was computed instead for probe copies. To perform the transcriptome investigation with the WGAA platform (Roche NimbleGen, http://www.roche.com), first- and second-strand cDNA synthesis, cDNA labeling, hybridization and washing steps were instead carried out according to the *NimbleGen Arrays User's Guide – Gene Expression Arrays* (version 5.1). Microarray slides were scanned at 532 nm (Cy3 absorption peak) using the Axon GenePix 4400A (Molecular Devices) and GenePix Pro 7 (Molecular Devices), according to the manufacturer's instructions. Feature extraction and robust multiarray average (RMA) normalization were performed using the specific software NimbleScan 2.5, with default parameters (Roche). For both iRIPE and WGAA platforms, DEGs were identified with linear model microarray analysis (LIMMA), assuming a false-discovery rate (FDR) < 0.05 and a $|\log 2(\text{fold change})| \geq 1$. The microarray design is extensively described in Appendix S2.

Eleven genes were further validated by real-time qPCR analysis, and 2 μg of total RNA from each sample was treated with 2 units of Ambion rDNAse I (DNA free kit; Life Technologies, now ThermoFisher Scientific), and then converted into cDNA using the 'Super-Script VILO cDNA Synthesis Kit' (Life Technologies). The assessment of the gene expression profiles was carried out using the FAST SYBR GREEN MASTER MIX (Life Technologies) and the ViiA7™ instrument (Life Technologies). The Ct (threshold cycle) results were calculated by averaging three independent normalized expression values for each sample. Relative gene expression was plotted as the mean of the normalized expression values using Q-gene (Muller *et al.*, 2002). The housekeeping gene employed for this investigation was Md8283 (Botton *et al.*, 2011). Primer 3 by SimGene was used to design primers for real-time PCR. The primer sequences for each target gene were reported in Table S9.

Data analysis is documented in Appendix S3.

Accession number

The data discussed in this publication have been deposited in the National Center for Biotechnology Information (NCBI) Gene Expression Omnibus (Edgar *et al.*, 2002), and are accessible through GEO series accession number GSE78746 (http://www.ncbi.nlm.nih.gov/geo/query/acc.cgi?acc=GSE78746).

ACKNOWLEDGMENTS

This work was supported by the CANDI-HAP project (Provincia Autonoma di Trento) and the Progetto Agroalimentare e Ricerca (grant no. 2010-2119). The authors are grateful to Justin Lashbrooke for a critical reading of this manuscript. The authors declare no conflicts of interest.

AUTHOR CONTRIBUTION

A.T. and S.L. performed the majority of the experiments; M.M. and A.F. provided bioinformatics assistance; P.T., A.M. and C.A. contributed to RNAseq and microarray hybridization; B.F., U.V., F.B., L.C. performed metabolite profiling, N.B. and M.S. contributed to data analysis; R.V. and M.D. provided assistance to the work; L.T. complemented the writing; F.C. conceived the research plan, supervised the experiments and wrote the article.

SUPPORTING INFORMATION

Additional Supporting Information may be found in the online version of this article.

Figure S1. Experimental designs for 'Golden Delicious' (A) and 'Granny Smith' (B).

Figure S2. Transcriptional profile clustering based on the self-organizing tree algorithm (SOTA).

Figure S3. Three snapshots of the expression dynamics during the fruit development and ripening of 'Golden Delicious'.

Figure S4. Venn diagram indicating the number of differentially expressed genes (DEGs) among the samples of 'Golden Delicious' assessed with the iRIPE platform.

Figure S5. Gene expression visualization based on MapMan view.

Figure S6. Expression profile comparison between RT-qPCR and the transcription pattern assessed with the two microarray platforms for 11 selected genes.

Figure S7. Comparison of the DEG inventory expressed for each stage of the time course in both 'Golden Delicious' and 'Granny Smith' apple cultivars.

Figure S8. HeatMap depicting the WGAA expression profile of cell wall related genes (S8a), ethylene related genes (S8b), auxin related elements (S8c) and transcription factors (S8d).

Figure S9. Correlation analysis network (CAN) for texture parameters (S9a) and VOCs (S9b).

Table S1. List of differentially expressed genes (DEGs) in the pairwise comparison among the stages of 'Golden Delicious', assessed with the iRIPE platform.

Table S2. List of differentially expressed genes (DEGs) detected in the comparison between H and PH_{CTRL} (a) and $PH_{CTRL/1\text{-}MCP}$ (b).

Table S3. Differentially expressed gene (DEG) comparison between GD and GS apple cultivars for MG (a), B (b), H (c), PH_{CTRL} (d) and $PH_{1\text{-}MCP}$ (e).

Table S4. Differentially expressed genes (DEGs) detected at stage H for both GD and GS apple cultivars and related to cell wall, ethylene, auxin and transcription factors.

Table S5. List of differentially expressed genes (DEGs) identified comparing the different samples of GD and related to cell wall (a and b), ethylene (c and d), auxin (e and f) and transcription factors (g and h).

Table S6. Correlation analysis network computed between iRIPE transcript and ethylene (CTRL and 1-MCP; a and b), mechanical parameters (CTRL and 1-MCP; c and d), acoustic parameters (CTRL and 1-MCP; e and f) and VOCs (CTRL and 1-MCP; g and h).

Table S7. Correlation between WGAA transcripts and ethylene (a), cell wall (b), VOCs (c) and polyphenolic compounds (d).

Table S8. List of texture parameters, for both mechanical (a) and acoustic components (b), obtained from the combined profile.

Table S9. List of oligos used for the RTqPCR validation.

Appendix S1. Phenomic characterization of fruit texture behavior and secondary metabolite production.

Appendix S2. Microarray design description.

Appendix S3. Data analysis.

REFERENCES

Adams, D.O. and Yang, S.F. (1979) Ethylene biosynthesis: identification of 1-aminocyclopropane-1-carboxylic acid as an intermediate in the conversion of methionine to ethylene. *Proc. Natl Acad. Sci.* **76**, 170–174.

Alagna, F., Mariotti, R., Panara, F. *et al.* (2012) Olive phenolic compounds: metabolic and transcriptional profiling during fruit development. *BMC Plant Biol.* **12**, 162.

Alba, R., Payton, P., Fei, Z., McQuinn, R., Debbie, P., Martin, G.B., Tanksley, S.D. and Giovannoni, J.J. (2005) Transcriptome and selected metabolite analyses reveal multiple points of ethylene control during tomato fruit development. *Plant Cell* **17**, 2954–2965.

Alexander, L. and Grierson, D. (2002) Ethylene biosynthesis and action in tomato: a model for climacteric fruit ripening. *J. Exp. Bot.* **53**, 2039–2055.

Barry, C.S., Llop-Tous, I. and Grierson, D. (2000) The regulation of 1-aminocyclopropane-1-carboxylic acid synthase gene expression during the transition from system-1 to system-2 ethylene synthesis in tomato. *Plant Physiol.* **123**: 979–986.

Bennett, A.B. and Labavitch, J.M. (2008) Ethylene and ripening-regulated expression and function of fruit cell wall modifying proteins. *Plant Sci.* **175**, 130–136.

Bleecker, A.B. and Kende, H. (2000) Ethylene: a gaseous signal molecule in plants. *Annu. Rev. Cell Dev. Biol.* **16**, 1–18.

Bleecker, A.B. and Schaller, G.E. (1996) The mechanism of ethylene perception. *Plant Physiol.* **111**, 653–660.

Botton, A., Eccher, G., Forcato, C. *et al.* (2011) Signaling pathways mediating the induction of apple fruitlet abscission. *Plant Physiol.* **155**, 185–208.

Breitling, R., Li, Y., Tesson, B.M. *et al.* (2008) Genetical Genomics: Spotlight on QTL Hotspots. PMID: 18949031

Carrara, S., Pardossi, A., Soldatini, G.F., Tognoni, F. and Guidi, L. (2001) Photosynthetic activity of ripening tomato fruit. *Photosynthetica*, **39**, 75–78.

Chapman, E.J. and Estelle, M. (2009) Mechanism of auxin-regulated gene expression in plants. *Annu. Rev. Genet.* **43**, 265–285.

Chaumont, F. and Tyerman, S.D. (2014) Aquaporins: highly regulated channels controlling plant water relations. *Plant Physiol.* **164**, 1600–1618.

Ciardi, J.A., Tieman, D.M., Lund, S.T., Jones, J.B., Stall, R.E. and Klee, H.J. (2000) Response to Xanthomonas campestris pv. vesicatoria in tomato involves regulation of ethylene receptor gene expression. *Plant Physiol.* **123**, 81–92.

Ciardi, J.A., Tieman, D.M., Jones, J.B. and Klee, H.J. (2001) Reduced expression of the tomato ethylene receptor gene LeETR4 enhances the hypersensitive response to Xanthomonas campestris pv. vesicatoria. *Mol. Plant Microbe Interact.* **14**, 487–495.

Costa, F., Alba, R., Schouten, H. *et al.* (2010) Use of homologous and heterologous gene expression profiling tools to characterize transcription dynamics during apple fruit maturation and ripening. *BMC Plant Biol.* **10**, 229.

Costa, F., Cappellin, L., Longhi, S. *et al.* (2011) Assessment of apple (*Malus x domestica* Borkh.) fruit texture by a combined acoustic-mechanical profiling strategy. *Postharvest Biol. Technol.* **61**, 21–28.

Costa, F., Cappellin, L., Fontanari, M., Longhi, S., Guerra, W., Magnago, P., Gasperi, F. and Biasioli, F. (2012) Texture dynamics during postharvest cold storage ripening in apple (*Malus x domestica* Borkh.). *Postharvest Biol. Technol.* **69**, 54–63.

Costa, F., Cappellin, L., Farneti, B., Tadiello, A., Romano, A., Soukoulis, C., Sansavini, S., Velasco, R. and Biasioli, F. (2014) Advances in QTL mapping for ethylene production in apple (*Malus* × *domestica* Borkh.). *Postharvest Biol. Technol.* **87**, 126–132.

Dandekar, A.A., Teo, G., Defilippi, B.G., Uratsu, S.L., Passey, A.J., Kader, A.A., Stow, J.R., Colgan, R.J. and James, D.J. (2004) Effect of down-regulation of ethylene biosynthesis on fruit flavour complex in apple fruit. *Transgenic Res.* **13**, 373–384.

Defilippi, B.G., Dandekar, A.M. and Kader, A.A. (2005) Impact of suppression of ethylene action or biosynthesis on flavour metabolites in apple (*Malus x domestica* Borkh.) fruits. *J. Agric. Food Chem.* **52**, 5694–5701.

Dillard, C.J. and German, J.B. (2000) Phytochemicals: nutraceuticals and human health. *J. Sci. Food Agric.* **80**, 1744–1756.

Ding, C.K., Chachin, K., Ueda, Y., Imahori, Y. and Wang, C.Y. (2001) Metabolism of phenolic compounds during loquat fruit development. *J. Agric. Food Chem.* **49**, 2883–2888.

Edgar, R., Domrachev, M. and Lash, A.E. (2002) Gene Expression Omnibus: NCBI gene expression and hybridization array data repository. *Nucleic Acids Res.* **30**, 207–210.

El-Ramady, H.R., Domokos-Szabolcsy, É., Abdalla, N.A., Taha, H.S. and Fári, M. (2015) Postharvest Management of Fruits and Vegetables Storage. In *Sustainable Agriculture Reviews vol 15* (Lichtfouse, E.,ed). Switzerland: Springer International Publishing, pp. 65–152.

Ezura, H. and Owino, W.O. (2008) Melon, an alternative model plant for elucidating fruit ripening. *Plant Sci.* **175**, 121–129.

Farneti, B., Busatto, N., Khomenko, I., Cappellin, L., Gutierrez, S., Spinelli, F., Velasco, R., Biasioli, F., Costa, G. and Costa, F. (2014) Untargeted metabolomics investigation of volatile compounds involved in the development of apple superficial scald by PTR-ToF–MS. *Metabolomics*, **11**, 341–349.

Giovannoni, J.J. (2001) Molecular biology of fruit maturation and ripening. *Annu. Rev. Plant Physiol. Plant Mol. Biol.* **52**, 725–749.

Giovannoni, J.J. (2007) Fruit ripening mutants yield insights into ripening control. *Curr. Opin. Plant Biol.* **10**, 283–289.

Guo, H. and Ecker, J.R. (2004) The ethylene signaling pathway: new insights. *Curr. Opin. Plant Biol.* **7**, 40–49.

Hackett, R.M., Ho, C.W., Lin, Z., Foote, H.C., Fray, R.G. and Grierson, D. (2000) Antisense inhibition of the Nr gene restores normal ripening to the tomato Never-ripe mutant, consistent with the ethylene receptor-inhibition model. *Plant Physiol.* **124**, 1079–1086.

Han, Y., Zhu, Q., Zhang, Z., Meng, K., Hou, Y., Ban, Q., Suo, J. and Rao, J. (2015) Analysis of xyloglucan endotransglycosylase/hydrolase (*XTH*) genes and diverse roles of isoenzymes during persimmon fruit development and postharvest softening. *PlosOne*, doi: 10.1371/journal.-pone0123668.

Hoang, N.T.T., Golding, J.B. and Wilkes, M.A. (2011) The effect of postharvest 1-MCP treatment and storage atmosphere on 'Cripps Pink' apple phenolics and antioxidant activity. *Food Chem.* **127**: 1249–1256.

Hyson, D.A. (2011) A comprehensive review of apples and apple components and their relationship to human health. *Adv Nutr.* **2**, 408–420.

Janssen, R.C. and Nap, J.-P. (2001) Genetical genomics: the added value from segregation. *Trends Genet.* **17**, 388–391.

Janssen, B.J., Thodey, K., Schaffer, R.L. *et al.* (2008) Global gene expression analysis of apple fruit development from the floral bud to ripe fruit. *BMC Plant Biol.* **8**, 16.

Jones, H.G. (1981) Carbon dioxide exchange of developing apple (Malus pumila Mill.) fruits. *J. Exp. Bot.* **32**, 1203–1210.

Joosen, R.V., Ligterink, W., Hilhorst, H.W. and Keurentjes, J.J. (2009) Advances in genetical genomics of plants. *Curr. Genomics* **10**, 540–549.

Kaur, C. and Kapoor, H.C. (2001) Antioxidants in fruits and vegetables – the millennium's health. *Int. J. Food Sci. Technol.* **36**, 703–725.

Klee, H.J. (2002) Control of ethylene-mediated processes in tomato at the level of receptors. *J. Exp. Bot.* **53**, 2057–2063.

Klee, H.J. and Giovannoni, J.J. (2011) Genetics and control of tomato fruit ripening and quality attributes. *Annu. Rev. Genet.* **45**, 41–59.

Kramer, M., Sanders, R., Bolkan, H., Waters, C., Sheehy, R.E. and Hiatt, W.R. (1992) Postharvest evaluation of transgenic tomatoes with reduced levels of polygalacturonase: processing, firmness and disease resistance. *Postharvest Biol. Technol.* **1**, 241–255.

Lanahan, M.B., Yen, H.C., Giovannoni, J.J. and Klee, H.J. (1994) The never ripe mutation blocks ethylene perception in tomato. *Plant Cell* **6**, 521–530.

Langley, K.R., Martin, A., Stenning, R., Murray, A.J., Hobson, G.E., Schuch, W.W. and Bird, C.R. (1994) Mechanical and optical assessment of the ripening of tomato fruit with reduced polygalacturonase activity. *J. Sci. Food Agric.* **66**, 547–554.

Leyser, O. (2010) The power of auxin in plants. *Plant Physiol.* **154**, 501–505.

Li, J. and Burmeister, M. (2005) Genetical genomics: combining genetics with gene expression analysis. *Hum. Mol. Genet.* **14**, R163–R169.

Liu, R.H. (2004) Potential synergy of phytochemicals in cancer prevention: mechanism of action. *J. Nutr.* **134**, 3479S–3485S.

Ljung, K. (2013) Auxin metabolism and homeostasis during plant development. *Development*, **140**, 943–950.

Lokerse, A.S. and Weijers, D. (2009) Auxin enters the matrix – assembly of response machineries for specific outputs. *Curr. Opin. Plant Biol.* **12**, 520–526.

Longhi, S., Moretto, M., Viola, R., Velasco, R. and Costa, F. (2012) Comprehensive QTL mapping survey dissects the complex fruit texture physiology in apple (*Malus x domestica* Borkh.). *J. Exp. Bot.* **63**, 1107–1121.

Longhi, S., Hamblin, M.T., Trainotti, L., Peace, C.P., Velasco, R. and Costa, F. (2013) A candidate gene based approach validates Md-PG1 as the main responsible for a QTL impacting fruit texture in apple (*Malus x domestica* Borkh.). *BMC Plant Biol.* **13**, 37.

Lytovchenko, A., Eickmeier, I., Pons, C. *et al.* (2011) Tomato fruit photosynthesis is seemingly unimportant in primary metabolism and ripening but plays a considerable role in seed development. *Plant Physiol.* **157**, 1650–1663.

Ma, N., Feng, H., Meng, X., Li, D., Yang, D., Wu, C. and Meng, Q. (2014) Overexpression of tomato *SlNAC1* transcription factor alters fruit pigmentation and softening. *BMC Plant Biol.* **14**, 351.

Matas, A.J., Gapper, N.E., Chung, M.Y., Giovannoni, J.J. and Rose, J.K.C. (2009) Biology and genetic engineering of fruit maturation for enhanced quality and shelf-life. *Curr. Opin. Biotechnol.* **20**, 197–203.

Maurel, C. (1997) Aquaporins and water permeability of plant membranes. *Annu Rev Pant Physiol Plant Mol Biol*, **48**, 399–429.

Morgan, P. and Hall, W. (1962) Effect of 2,4-dichlorophenoxyacetic acid on the production of ethylene by cotton and grain sorghum. *Physiol Plantarum*, **15**, 420–427.

Muday, G.K., Rahman, A. and Binder, B.M. (2012) Auxin and ethylene: collaborators or competitors? *Trends Plant Sci.* **17**, 1360–1385.

Muller, P.Y., Janovjak, H., Miserez, A.R. and Dobbie, Z. (2002) Processing of gene expression data generated by quantitative real-time RT-PCR. *Biotechniques*, **32**, 1372–1378.

Mut, P., Bustamante, C., Martinez, G., Alleva, K., Sutka, M., Civello, M. and Amodeo, G. (2008) A fruit-specific plasma membrane aquaporin subtype PIP1;1 is regulated during strawberry (*Fragaria x ananassa*) fruit ripening. *Physiol Plantarum*, **132**, 538–551.

Nishitani, K. (1995) Endo-xyloglucan transferase, a new class of transferase involved in cell wall construction. *J. Plant. Res.* **108**, 137–148.

Nishitani, K. and Tominaga, R. (1992) Endo-xyloglucan transferase, a novel class of glycosyltransferase that catalyzes transfer of a segment of xyloglucan molecule to another xyloglucan molecule. *J. Biol. Chem.* **267**, 21058–21064.

Nishiyama, K., Guis, M., Rose, J.K.C. *et al.* (2007) Ethylene regulation of fruit softening and cell wall disassembly in Charentais melon. *J. Exp. Bot.* **58**, 1281–1290.

Nyasordzi, J., Friedman, H., Schmilovitch, Z., Ignat, T., Weksler, A., Rot, I. and Lurie, S. (2013) Utilizing the IAD index to determine internal quality attributes of apples at harvest and after storage. *Postharvest Biol. Technol.* **77**, 80–86.

Osorio, S., Alba, R., Damasceno, C.M. *et al.* (2011) Systems biology of tomato fruit development: combined transcript, protein, and metabolite analysis of tomato transcription factor (nor, rin) and ethylene receptor (Nr) mutants reveals novel regulatory interactions. *Plant Physiol.* **157**, 405–425.

Osorio, S., Alba, R., Nikoloski, Z., Kochevenko, A., Fernie, A.R. and Giovannoni, J.J. (2012) Integrative comparative analyses of transcript and metabolite profiles from pepper and tomato ripening and development stages uncovers species-specific patterns of network regulatory behavior. *Plant Physiol.* **159**, 1713–1729.

Pech, J.C., Bouzayen, M. and Latche, A. (2008) Climacteric fruit ripening: ethylene-dependent and independent regulation of ripening pathways in melon fruit. *Plant Sci.* **175**, 114–120.

Reuscher, S., Akiyama, M., Mori, C., Aoki, K., Shibata, D. and Shiratake, K. (2013) Genome-wide identification and expression analysis of aquaporins in tomato. *PlosOne*, **8**, e79052, 1–13.

Ritchie, M.E., Phipson, B., Wu, D., Hu, Y., Law, C.W., Shi, W. and Smyth, G.K. (2015) Limma powers differential expression analyses for RNA-sequencing and microarray studies. *Nucleic Acid Res.* **43**, e47.

Rohrmann, J., Tohge, T., Alba, R. *et al.* (2011) Combined transcription factor profiling, microarray analysis and metabolite profiling reveals the transcriptional control of metabolic shifts occurring during tomato fruit development. *Plant J.* **68**, 999–1013.

Rose, J.K.C., Hadfield, K.A., Labavitch, J.M. and Bennett, A.B. (1998) Temporal sequence of cell wall disassembly in rapidly ripening melon fruit. *Plant Physiol.* **117**, 345–361.

Schaffer, R.J., Friel, E.N., Souleyre, E.J.F. *et al.* (2007) A genomics approach reveals that aroma production in apple is controlled by ethylene predominantly at the final step in each biosynthetic pathway. *Plant Physiol.* **144**, 1899–1912.

Schaffer, R.J., Ireland, H.S., Ross, J.J., Lingm, T.J. and David, K.M.. (2013). SEPALLATA1/2-suppressed mature apples have low ethylene, high auxin and reduced transcription of ripening-related genes. *AoB Plants* **5**, pls047–pls047.

Shin, S., Lee, J., Rudell, D., Evans, K. and Zhu, Y.. 2016. Transcriptional Regulation of Auxin Metabolism and Ethylene Biosynthesis Activation During Apple (Malus × domestica) Fruit Maturation. *J. Plant Growth Regul.* **35**, 655–666.

Sisler, E.E. and Serek, M. (1997) Inhibitors of ethylene responses in plants at the receptor level: recent developments. *Physiol Plantarum*, **100**, 577–582.

Sitrit, Y. and Bennett, A.B. (1998) Regulation of tomato fruit polygalacturonase mRNA accumulation by ethylene: a re-examination. *Plant Physiol.* **116**, 1145–1150.

Soglio, V., Costa, F., Molthoff, J.W., Weemen-Hendriks, W.M.J., Schouten, H.J. and Gianfranceschi, L. (2009) Transcription analysis of apple fruit development using cDNA microarrays. *Tree Genet and Gen* **5**, 685–698.

Tieman, D.M., Taylor, M.G., Ciardi, J.A. and Klee, H.J. (2000) The tomato ethylene receptors NR and LeETR4 are negative regulators of ethylene response and exhibit functional compensation within a multigene family. *PNAS* **97**, 5663–5668.

Tohge, T., Alseekh, S. and Fernie, A.R. (2014) On the regulation and function of secondary metabolism during fruit development and ripening. *J. Exp. Bot.* **65**, 4599–4611.

Trainotti, L., Tadiello, A. and Casadoro, G. (2007) The involvement of auxin in the ripening of climacteric fruits comes to age: the hormone plays a role of its own and has an intense interplay with ethylene in ripening peaches. *J. Exp. Bot.* **58**, 3299–3308.

Vrhovsek, U., Masuero, D., Gasperotti, M., Franceschi, P., Caputi, L., Viola, R. and Mattivi, F. (2012) A versatile targeted metabolomics method for the rapid quantification of multiple classes of phenolics in fruits and beverages. *J. Agric. Food Chem.* **60**, 8831–8840.

Wang, K.L.C., Li, H. and Ecker, J.R. (2002) Ethylene biosynthesis and signaling networks. *Plant Cell* **14**, S131–S151.

Xie, Q., Frugis, G., Colgan, D. and Chua, N.H. (2000) *Arabidopsis* NAC1 transduces auxin signal downstream of TIR1 to promote lateral root development. *Genes Dev.* **14**, 3024–3036.

Yang, S.F. and Hoffman, N.E. (1984) Ethylene biosynthesis and its regulation in higherplants. *Annu Rev Plant Physiol*, **35**, 155–189.

Zhu, Y., Zheng, P., Varanasi, V., Shin, S., Main, D., Curry, E. and Mattheis, J.P. (2012) Multiple plant hormones and cell wall metabolism regulate apple fruit maturation patterns and texture attributes. *Tree Genet and Gen* **8**, 1389–1406.

Zhu, M., Chen, G., Zhou, S., Tu, Y., Wang, Y., Dong, T. and Hu, Z. (2014) A new tomato NAC (NAM/ATAF1/2/CUC2) transcription factor, SlNAC4, functions as a positive regulator of fruit ripening and carotenoid accumulation. *Plant Cell Physiol.* **55**, 119–135.

